Journal Name

ARTICLE

# Fluorination induced electronic effects on Pt(II) square-planar complex of *o*-phenylenediimine ligand

Received 00th January 20xx,
Accepted 00th January 20xx

DOI: 10.1039/x0xx00000x

www.rsc.org/

L. Pilia,[*ab] M. M. Matsushita,[c] K. Awaga[c] and N. Robertson[b]

The novel complex [Pt($C_6F_4(NH)_2$)$_2$] (**2**), formed by a Pt(II) cation bound to two molecules of the tetrafluorinated 1,2-phenylenediimine ligand, has been synthesized and characterized by electrochemical and XRD measurements, UV-Vis-NIR spectroscopy as well as by DFT and TD-DFT calculations. The effect induced by the fluorine atoms has been highlighted by comparison with the corresponding Ni (**1H**) and Pt (**2H**) hydrogenated complexes. The cyclic voltammetry data show that the reduction and the oxidation processes of **2** are easier and more difficult (by about 0.5 V), respectively, compared to those of **1H** and **2H**, suggesting that the electron withdrawing capability of the fluorine atoms lowers the energy level of both HOMO and LUMO orbitals. UV-vis-NIR measurements are similar for all the three complexes, indicating similar HOMO-LUMO gaps and that the effects of the fluorination on the frontier orbitals are roughly the same. Moreover, polymorphism in the powder form of **2** has been highlighted by XRD measurements while the film presents only one phase. Furthermore, this complex shows field-effect for *n*-type carriers. All the experimental results are also supported by the calculations, which show the role played by the fluorine atoms in the electronic structure of **2**.

## Introduction

Extended studies have been devoted in the last decades to molecular semiconductors (MSC) with the aim to use them as active materials in devices for many electronic and optoelectronic applications.[1] Their easy processability by vapour deposition or from solution, which makes these compounds suitable to prepare cheap, large-area, thin films, in addition to their flexibility, explains the technological interest on these compounds.[1] In comparison with the hole-conducting (*p*-type) MSC, the number of *n*-type (electron carriers) systems reported is much smaller;[2] moreover, the majority of them are not air-stable. Previously reported studies have shown that, in operational conditions and exposed to the air, a *n*-type MSC is stable if it presents a first reduction peak at potential more positive than −0.66 V (*vs.* SCE),[3] corresponding to a lowest unoccupied molecular orbital (LUMO) energy level deeper than −4 eV.[2g]

In silicon technology, complementary circuits, which perform better than unipolar circuits, are prepared using discrete *p*- and *n*-channel transistors; however, this architecture is not appropriate for MSC systems.[4a] A different manner to prepare integrated devices suitable for this kind of semiconductors, is the complementary-like technology. Proposed by Anthopoulos and coworkers, this approach is based on ambipolar transistors.[4] The active layer in this kind of device is formed by a SC which shows injection and transport properties for both holes and electrons. In order to present balanced mobilities for the two types of carriers, the SC should have a relatively-small HOMO-LUMO energy gap (HOMO = highest occupied molecular orbital). Moreover, a narrow-band-gap is suitable in order to avoid sizable charge injection barriers when the same metal is used for both the drain and source electrodes, reducing the devices' production costs.

So far, several metal complexes were proposed as semiconductor for field-effect transistors (FET) applications.[2e,2g-k] The nickel(II) complex [Ni($C_6H_4(NH)_2$)$_2$] (**1H**) ($C_6H_4(NH)_2^-$ = *o*-diiminobenzosemiquinonate) in DMF solution presents a reduction process and an oxidation process, both reversible, at −1.37 and −0.36 V, respectively against NHE.[5a] The energy levels of the frontier orbitals (FOs) were estimated as −3.43 eV for the LUMO and −4.44 eV in the case of the HOMO, with a small HOMO-LUMO gap of 1.03 eV.[5] Furthermore, in a metal-organic thin film transistor (MOTFT) device with gold electrodes, **1H** exhibits a hole mobility of $3.8{\cdot}10^{-2}$ $cm^2$ $V^{-1}$ $s^{-1}$, while it does not show any electron mobility; therefore, despite its small HOMO-LUMO gap, in this kind of transistor no ambipolar behaviour can be observed for **1H**.[5a] These findings were explained with the electron trapping effect due to the presence of silanol groups (SiOH) on the dielectric ($SiO_2$) surface,[5b, 6] and with the mismatch between

[a] Dipartimento di Ingegneria Meccanica Chimica e dei Materiali, Università di Cagliari, via Marengo 2, I09123, Cagliari, Italy.
[b] School of Chemistry and EaStChem, University of Edinburgh, King's Buildings, David Brewster Road, Edinburgh EH9 3FJ, UK.
[c] Department of Chemistry, Graduate School of Science, and Research Center of Materials Science Nagoya University, Chikusa-ku, Nagoya 464-8602, Japan.

† Footnotes relating to the title and/or authors should appear here.

Electronic Supplementary Information (ESI) available: Chart S1 and Table S1; Cyclic voltammograms (Figures S1-S5); DFT calculations: optimized geometries (Figure S6), Tables S2-S6 and FOs of 1H (Figure S7); Energy levels diagram (Figure S8); TD-DFT calculated electronic spectra (Figures S9 and S10); XRD patterns (Figures S11 and S12); FET measurements (Figures S13). See DOI: 10.1039/x0xx00000x

the gold work function (w.f.$_{Au}$ = –5.1 eV) and the LUMO energy which makes the injection of electrons difficult.[5b] In order to overcome the first issue, a layer of a hydroxyl-free polymer, poly-methylmethacrylate (PMMA), was placed into the MOTFT between the semiconductor and $SiO_2$. Ambipolar behaviour with mobilities of $2.3{\cdot}10^{-4}$ and $4.0{\cdot}10^{-6}$ $cm^2\ V^{-1}\ s^{-1}$ for hole and electron, respectively, was observed with Au electrodes. Calcium electrodes (w.f.$_{Ca}$ = –2.9 eV) were also used instead of the gold ones to reduce the electron injection barrier, giving better balance between the two types of carriers and higher mobilities ($4.3{\cdot}10^{-3}$ $cm^2\ V^{-1}\ s^{-1}$ for hole and $1.6{\cdot}10^{-2}$ $cm^2\ V^{-1}\ s^{-1}$ for electron).[5b]

With the aim to obtain an air stable ambipolar SC, which will avoid the deposition of the OH-free polymer into the device, we have prepared the Pt(II) complex of the corresponding tetrafluorinated ligand, the $[Pt(C_6F_4(NH)_2)_2]$ (**2**). In the present paper, the effects induced by the fluorine atoms in the properties of this complex, will be highlighted by comparison with **1H** and with the analogous non-fluorinated Pt-complex (**2H**),[7] which shows electrochemical and optical properties very similar to those presented by the corresponding Ni one.

## Experimental section

All the reagents and solvents were purchased from Aldrich and used without further purification. The ligand 3,4,5,6-tetrafluoro-1,2-phenylenediamine ($C_6F_4(NH_2)_2$) was prepared as previously described by Heaton *et al.*.[8]

### Preparation

$[Pt(C_6F_4(NH)_2)_2]$ (**2**). *Synthesis*: complex **2** has been prepared by modifying the procedure reported by Balch *et al*. for the homologous not-fluorinated compound.[7a] 600 mg (3.12 mmol) of $C_6F_4(NH_2)_2$ and 414 mg (1.56 mmol) of $PtCl_2$ were mixed in 300 mL of methanol and the solvent colour immediately turned green; the resulting suspension was refluxed under stirring overnight. The solution was filtered and its volume halved by evaporation; then, after the addition of water, a blue-purple solid, which was collected by filtration and recrystallized in hot MeOH (92 mg), appeared. The addition of few drops of $NH_3$ 28% to the water/methanol mother liquor was followed by precipitation of a blue-purple solid which was collected by filtration and washed 4 times with methanol (690 mg). Total yield 782 mg, 1.42 mmol; 91%). Analytical results are in accordance with the formula $[Pt(C_6F_4(NH)_2)_2]$. Elemental Analysis: calculated for $C_{12}H_4F_8N_4Pt$ (551.25): C 26.15, H 0.73, N 10.16; found: C 25.98, H 0.80, N 10.21. MS (EI): m/z (%) 550.10 (100.00%) $[M–H]^-$. UV-vis [in $CH_2Cl_2$; $\lambda$, nm ($\varepsilon$, $dm^3{\cdot}mol^{-1}{\cdot}cm^{-1}$)]: 715, sh; 688 ($7.63{\cdot}10^4$); 644, sh; 564, sh; 304 ($4.81{\cdot}10^3$). FT–IR (KBr): $\nu_{max}/cm^{-1}$ 3389(vs); 1635(mw); 1529(s); 1499(ms); 1419(m); 1384(ms); 1357(vs); 1258(ms); 1124(w); 1062(vw); 1001(m); 869(vw); 802(vw); 737(vw); 675(mw); 653(w); 495(vw); 455(w); 409(vw).

Elemental Analyses were performed with a Carlo Erba CE1108 Elemental Analyser. MS were recorded on ThermoElectron MAT 900 by electron impact (EI) ionization technique. The UV-vis-near-IR spectra were measured with a Jasco V-670 spectrophotometer equipped with a diffuse reflectance accessory. In solution they were recorded using a quartz cell of path length 1 cm, those in diffuse reflection mode were run on KBr pellets. IR measurements (4000-400 $cm^{-1}$) were performed with a spectrophotometer FT-IR Bruker Tensor27 on KBr pellets. Cyclic voltammograms were carried out using an μAUTOLAB Type III potentiostat, driven by the GPES electrochemical software; employing a conventional three-electrode cell consisting of a platinum wire working electrode, a platinum wire as counter-electrode and Ag/AgCl in a 3.0 $mol{\cdot}dm^{-3}$ KCl solution as reference electrode. The experiments were performed at room temperature (25°C), in dry and degassed DMF or THF or $CH_2Cl_2$ containing 0.1 mol $dm^{-3}$ $Bu_4NPF_6$ as supporting electrolyte, at 25-200 mV $s^{-1}$ scan rate. Data are quoted against ferrocene/ferrocenium couple (internal standard); under the above conditions the half-wave potentials for $Fc/Fc^+$ are +0.574 V in DMF, +0.79 V in THF and +0.53 V in $CH_2Cl_2$ against NHE.

### DFT calculations

Ground-state electronic structure calculations of **2** were performed at Density Functional Theory (DFT)[9] level employing the GAUSSIAN 09[10] software package. The functional used throughout this study was B3LYP.[11] The ground state geometries were obtained in the gas phase by full geometry optimization without any symmetry constraint. The basis set employed for all atoms was the valence triple-zeta 6-311+G(d,p).[12] All structures were input through ArgusLab 4.0 program.[13] The atomic orbital compositions were calculated using a Simple Contribution Analysis. The effects of solvation on the complexes were taken into account using the Polarizable Continuum Model (PCM); the ground state geometry was optimized in a $CH_2Cl_2$ simulated electric field ($\varepsilon$ = 8.93). The 10 lowest singlet excited states of the closed shell complexes were calculated within the time-dependent DFT (TD-DFT) formalism as implemented in Gaussian,[14] both, in the gas phase and in $CH_2Cl_2$. The optimized molecular structures and the orbital isosurfaces were visualized using ArgusLab 4.0.[13]

### Film growth

Deposition of **2** thin films for XRD (on Si(100)) and FET characterizations was carried out via physical vapor deposition (PVD) with sources held in a temperature between 211 ºC and 213 ºC at a pressure of $2.4{\cdot}10^{-4}$ Pa. The growth rate, which resulted in a of 0.1-0.2 Å $s^{-1}$, was monitored using a quartz crystal microbalance. Films of 80 nm thickness were produced according to the QCM. The actual film thickness (45±5 nm) was measured using a profilometer. FET substrates with platinum drain and source electrodes with gap and width of 2 μm, have been used. The measurements were carried out in darkness and under vacuum using a Keithley 2636A sourcemeter equipped with Labtracer 2.0 software.

### XRD characterization

Powder XRD spectra were recorded with a Panalytical Empyrean diffractometer equipped with a graphite monochromator and a X'Celerator linear detector. Data were collected within the range 3–90° (2θ) using Cu Kα radiation. Thin film XRD was measured on a Rigaku ultraX-18HB at room temperature. The scans were collected from 2θ angle of 3–80° at a rate of 3° per minute in the out of plane mode

## Results and discussion

Complex **2** has been prepared in a good yield, by mixing the 3,4,5,6-tetrafluoro-1,2-phenylenediamine ($C_6F_4(NH_2)_2$) ligand and $PtCl_2$ in methanol/water solution with the addition of few drops of concentrated ammonia. Attempts to prepare the analogous Ni complex following the method described above, as well as that reported for **1H**,[7a] lead to the desired product in a very low yield; further experiments will be done in order to prepare this complex in a satisfactory yield.

### Electrochemical studies

The cyclicvoltammogram of **2** (Figure 1) in DMF presents (*vs* $Fc^+/Fc$) two reversible peaks at 0.21 ($i_c/i_a$ = 0.77) and –0.99 V ($i_c/i_a$ = 0.93), corresponding to the oxidation (0 ⇌ +1) and reduction (0 ⇌ –1) processes, respectively, and a partially reversible reduction waves at –1.73 V (–1 → –2). Measures performed in DCM and THF show an additional peak relatable to the +1 to +2 oxidation process (see Figure S4 and S5), which is not observed in DMF, probably because it falls out of the window of stability of the solvent. Complex **2H** exhibits four reversible redox processes falling at values shifted by about 0.5 V toward more negative potentials compared with those of **2**.[7] The presence of fluorine atoms at the benzene ring lowers the energy of the FOs, making the reductions and the oxidations of **2** easier and more difficult, respectively, compared to those of **2H**, which fall at –0.32 and –1.50 V (*vs* $Fc/Fc^+$) for the processes 0 ⇌ +1 and 0 ⇌ –1, respectively,[7] close to those observed for **1H**. The energies of the FO can be estimated from the electrochemical data[3,15] obtaining –5.02 eV for the HOMO and –3.81 eV for the LUMO, with a low gap of 1.21 eV. Calculated by the same method, the FOs' energies are –4.44 and –3.43 eV for HOMO and LUMO, respectively in the case of **1H**, and –4.48 eV for the HOMO and –3.33 eV for the LUMO for **2H**. Therefore, the fluorination seems to stabilize both the FOs in similar manner (–0.5 eV).

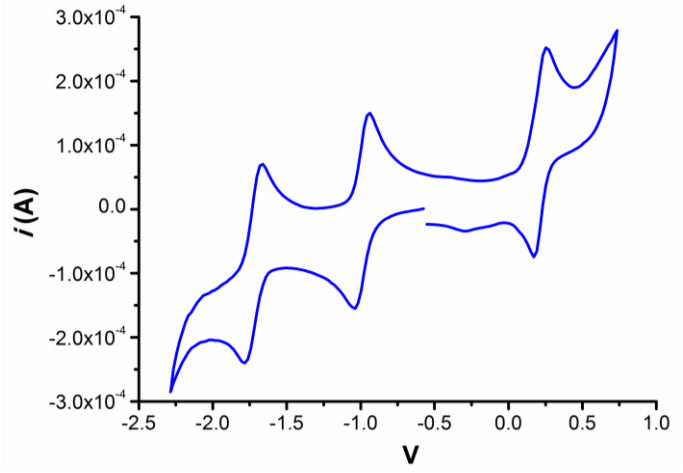


**Figure 1.** Cyclic voltammetry of **2** measured at the Pt electrode in a DMF degassed solution (V *vs* $F_c/F_c^+$).

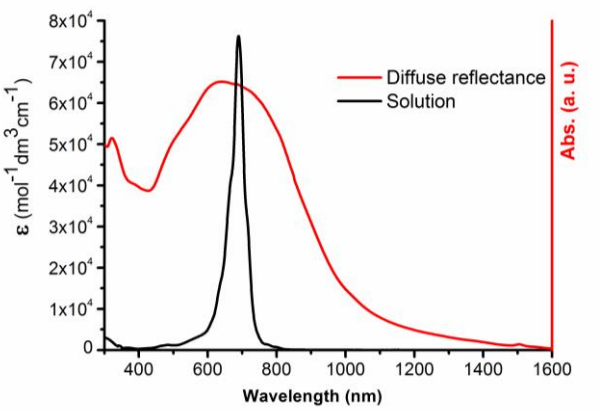


**Figure 2.** Comparison between $CH_2Cl_2$ solution and diffuse reflectance spectra of **2**.

### UV-vis-NIR measurements

The solution UV-vis-NIR spectrum of **2** in DCM is reported in Figure 2. A medium-intense ($dm^3 \cdot mol^{-1} \cdot cm^{-1}$) band falling at 304 ($4.81 \cdot 10^3$) in addition to an intense absorption at 688 nm ($7.63 \cdot 10^4$), is present. The latter band has been related to a HOMO-LUMO transition by TD-DFT calculations (*vide infra*). Similar spectra are shown by **1H**[5a] and **2H**,[7] with the maximum of the main absorption at 790 ($5.50 \cdot 10^4$) and 711 nm ($9.60 \cdot 10^4$), respectively.[7a] The HOMO-LUMO gap estimated from the onset of the related absorption (≅ 770 nm), shows a value of 1.61 eV. In Figure 2 is also depicted the UV-vis-NIR spectrum of **2** recorded in diffuse reflectance mode. A strong enlargement of the main band is observed, suggesting that strong intermolecular interactions, which are of paramount importance for conducting properties, occur in the solid state. A very narrow optical band-gap, of about 0.8 eV, is evaluated from the edge of the NIR absorption (≅ 1550 nm), in strong agreement with that found for a thin film of **1H**.[5]

### Computational studies

DFT calculations using B3LYP and 6-311+G(d,p) as functional and basis set, respectively, were performed in order to study the electronic structures of **1H**, **2** and **2H**. As expected, their gas-phase optimized geometry (Figure S6) are planar. A comparison between the FOs **2** and **2H** calculated in the same conditions is shown in Figure 3. The shapes of the corresponding molecular orbitals in the two complexes are similar, and both HOMOs and LUMOs present a $\pi$-symmetry with an electronic delocalization extended over the whole ligands.

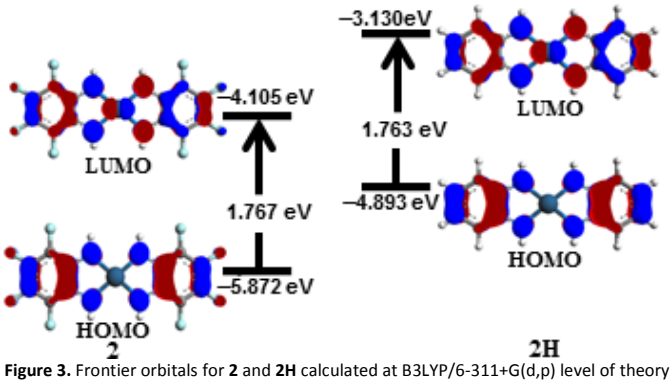


**Figure 3.** Frontier orbitals for **2** and **2H** calculated at B3LYP/6-311+G(d,p) level of theory and plotted with a contour value of 0.040.

Despite the relatively small contribution, the effect of the fluorination (see Tables S2 and S3) on the molecular orbitals' (MOs) energy levels is significant. The MOs of the complex bearing the halogen atoms are deeper in energy by about 1 eV comparing to the corresponding ones in the compound with hydrogen (Figure 3 and Table S4). The induced stabilization is almost the same for both FOs and consequently, the HOMO-LUMO gap is very similar in the two complexes, consistent with the likeness found in the electronic spectra (Table S5). The alteration of the electronic charge distribution induced by the presence of fluorine atoms instead of those of hydrogen, is clearly apparent in the Figure 4, where the electrostatic potential mapped on electron density isosurfaces is reported for both complexes: the fluorine atoms draw electronic density from throughout the molecule. The role played by the central metal has been investigated by performing calculation for **1H** (Figure S7). Compared to the corresponding platinum complex (Tables S5 and S6), the nickel one presents a smaller gap between the FOs due to a slight stabilization of the LUMO (by about 0.13 eV) and a small increase of the HOMO energy (≅0.10 eV). This finding is in accordance with the trend observed for the maxima absorptions in the vis-NIR region. Interestingly, the calculated LUMO energy of **2** (–4.105 eV) is lower than the maximum value (see above) required for this complex to be suitable to form air-stable *n*-type SC. Furthermore, in addition to other similarities, the small HOMO-LUMO gap close to that found for **1H**, makes **2** a good candidate for an ambipolar MSC.

The solvation effects of dichloromethane on the electronic structures of complexes **2** and **2H** were evaluated by PCM method (Figure S8 and Tables S3-S5). The effect of the solvent is opposite in the two complexes; indeed, it stabilizes the MOs in the case of **2H**, whereas it causes an increase of the energy of those of **2**.

The electronic transitions of **2** and **2H** were investigated by time-dependent (TD)-DFT calculations, in both gas phase and $CH_2Cl_2$ solution (Figures S9 and S10). The experimental maxima of the main bands are well predicted by the calculations ($662_{(calc.)}$ *vs* $688_{(exp.)}$ nm and $675_{(calc.)}$ *vs* $710_{(exp.)}$ nm for **2** and **2H**, respectively). Furthermore, on the basis of this TD-DFT study, the absorptions at lowest energy can be assigned to a HOMO-LUMO transition in both compounds.

### XRD measurements

The XRD pattern of the film of **2** grown onto a Si wafer by PVD is reported in Figure 5 along with that of the corresponding pristine powder. The comparison shows that all the peaks present in the spectrum of the film are also exhibited by that

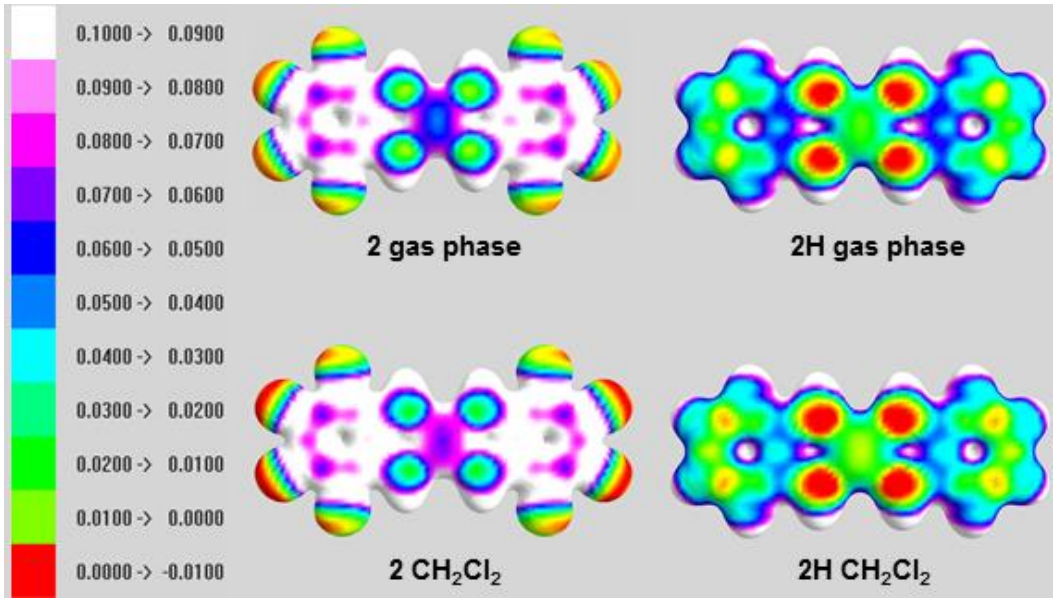


**Figure 4.** Electrostatic potential mapped on electron density isosurfaces, calculated by DFT (contour plot 0.020) for **2** and **2H** complexes. The colors are mapped according to the electrostatic potential at the point in space on the isosurface.

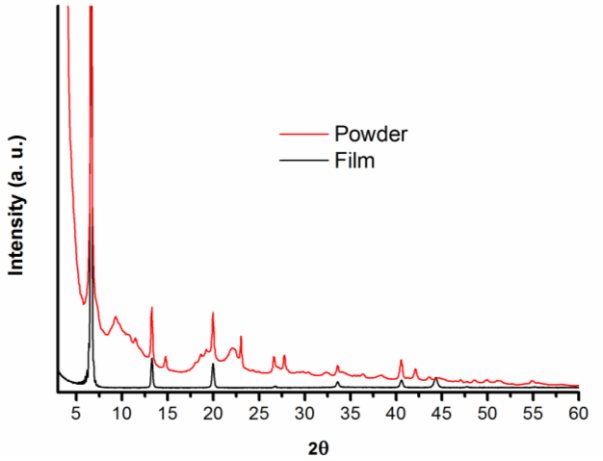


**Figure 5.** Comparison between the XRD spectrum of **2** deposited onto Si (black line) and that of the corresponding pristine powder (red line).

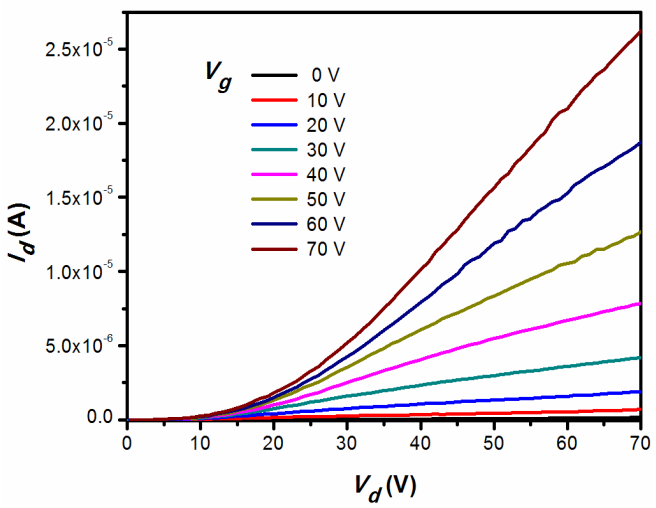


**Figure 6.** Output characteristics of **2** measured on substrates with Pt electrodes with gap and width of 2 μm.

of the powder. The additional peaks present in the latter pattern might be due to a preferential orientation of the molecules in the film and also to the presence of two different crystalline phases in the powder sample. Indeed, the comparison between the pattern of the pristine powder of the film and that of a sample obtained by slow evaporation from $CH_2Cl_2$ solution (see Figure S11) suggests the presence of a mixture of the two phases, in different ratios, in both samples. Two different crystallographic phases were also observed for complex **2H**.[16]

### FET measurements

Preliminary FET measurements have been performed on devices consisting of a substrate with source and drain interdigitated platinum electrodes with gap and width of 2 μm. The complex **2** clearly shows FET effects for *n*-type carriers (see Figure 6) in agreement with the calculation results (see above) and likewise some dithiolene complexes with similar FOs' energy levels and gaps.[2i] The electron-mobility, estimated from the transfer characteristics, is $4.0 \cdot 10^{-8}$ $cm^2$ $V^{-1}s^{-1}$, whereas the threshold voltage and on/off ratio are 26 V and $1 \cdot 10^3$, respectively. Moreover, the output characteristics of **2** did not present clear saturation region. This feature could be attributed to the relatively large Vg for Vd and the presence of Schottky barriers due to the mismatching between the work function of Pt and the LUMO level of **2**. The low field-effect electron-mobility observed in the FET device of **2** could be also explained in terms of the contribution of the Schottky barriers due to the high contact resistance at the electrode-semiconductor interface.

As mentioned in the Introduction, when the FET properties of **1H** were measured in devices with untreated dielectric ($SiO_2$) surface (like in the case of **2**) it shows a *p*-type behaviour, with a hole mobility of $3.8 \cdot 10^{-2}$ $cm^2$. While, when a layer PMMA is deposited between the active layer and $SiO_2$, in order to prevent the electron trapping effect, **1H** behaves as an ambipolar semiconductor with mobilities of $4.0 \cdot 10^{-6}$ and $2.3 \cdot 10^{-4}$ $cm^2$ $V^{-1}$ for electron and hole, respectively.[5b] The fact that for complex **2** the layer of PMMA is not required to show *n*-type conductivity, seems relatable with the stabilization of the energy levels due to the fluorination. The FET properties of **2H** have not been reported in the literature so far.

## Conclusions

A novel Pt(II) complex (**2**) of the tetrafluorinated 1,2-phenylenediimine ligand, has been prepared and characterized in order to investigate the effect induced by the substitution of the hydrogen atoms with fluorine, by comparison with the corresponding Ni (**1H**) and Pt (**2H**) hydrogenated complexes. The electrochemical data show that the electron withdrawing capability of the fluorine atoms lowers the energy level of both HOMO and LUMO orbitals. As a consequence, the reduction and the oxidation processes of **2** are easier and more difficult, respectively, compared to those of **1H** and **2H**. UV-vis-NIR measurements are similar for all the three complexes, suggesting similar HOMO-LUMO gaps and that the stabilization due to the fluorination is roughly the same for both of the FOs. Moreover, DFT calculations are in agreement with the experimental results. XRD studies show that **2** in the powder form exhibits two phases in different ratios, depending on the preparation route, whereas only one of these phases is present in the deposited film. Furthermore, **2** is a rare example of a metal complex clearly showing an FET effect in *n*-channel. The absence of the saturation region in the output characteristics of **2** suggests that further improvements in FET performance can be obtained with attention to the device architecture, electrode choice and film growth conditions.

## Acknowledgements

L. P. thanks the FP-7 PEOPLE-Marie Curie Intra European Programme and gratefully acknowledges Sardinia Regional Government for the financial support (P.O.R. Sardegna F.S.E. Operational Programme of the Autonomous Region of

Sardinia, European Social Fund 2007-2013 - Axis IV Human Resources, Objective l.3, Line of Activity l.3.1 “Avviso di chiamata per il finanziamento di Assegni di Ricerca”). We thank the EaStChem Research Computing Facility (http://www.eastchem.ac.uk/rcf). Funds were also provided by the JSPS Core-to-Core Program, A. Advanced Research Networks and the Leverhulme Trust to support the UK-Japan collaboration. The authors also thank Dr. Danilo Loche and Prof. Maria F. Casula for performing powder XRD measurements.

## Notes and references

1 (a) S.-S. Sun and L. R. Dalton, Introduction to Organic Electronic and Optoelectronic Materials and Devices; CRC Press: New York, 2008; (b) Z. Bao, *Adv. Mater.*, 2000, **12**, 227; (c) H. E. Katz, Z. Bao and S. L. Gilat, *Acc. Chem. Res.*, 2001, **34**, 359; (d) C. D. Dimitrakopoulos and P. R. L. Malenfant, *Adv. Mater.*, 2002, **14**, 99.

2 (a) X. Guo, A. Facchetti and T. J. Marks, *Chem. Rev.*, 2014, **114**, 8943; (b) B. Sun, W. Hong, Z. Yan, H. Aziz and Y. Li, *Adv. Mater.*, 2014, **26**, 2636; (c) J. E. Anthony, A. Facchetti, M. Heeney, S. R. Marder and X. Zhan, *Adv. Mater.* 2010, **22**, 3876; (d) B. A. Jones, A. Facchetti, M. R. Wasielewski and T. J. Marks, *J. Am. Chem. Soc.*, 2007, **129**, 15259; (e) Z. Bao, A. J. Lovinger, J. Brown, *J. Am. Chem. Soc.*, 1998, **120**, 207; (f) H. E. Katz, A. J. Lovinger, J. Johnson, C. Kloc, T. Seigrist, W. Li, Y.-Y. Lin, A. Dodabalapur, *Nature*, 2000, **404**, 478; (g) T. D. Anthopoulos, G. C. Anyfantis, G. C. Papavassiliou, and D. M. de Leeuw, *Appl. Phys. Lett.*, 2007, **90**, 122105; (h) G. C. Papavassiliou, G. C. Anyfantis and G. A. Mousdis, *Crystals*, 2012, **2**, 762; (i) J.-Y. Cho, B. Domercq, S. C. Jones, J. Yu, X. Zhang, Z. An, M. Bishop, S. Barlow, S. R. Marder and B. Kippelen, *J. Mater. Chem.*, 2007, **17**, 2642; (j) T. Taguchi, H. Wada, T. Kambayashi, B. Noda, M. Goto, T. Mori, K. Ishikawa and H. Takezoe, *Phys. Chem. Lett.*, 2006, **421**, 395; (k) L. Qu, Y. Guo, H. Luo, C. Zhong, G. Yu, Y. Liu and J. Qin, *Chem. Commun.*, 2012, **48**, 9965.

3 D. M. de Leeuw, M. M. J. Simenon, A. R. Brown and R. E. F. Einerhand, *Synth. Met.*, 1997, **87**, 53.

4 (a) T. D. Anthopoulos, S. Setayesh, E. Smits, M. Cölle, E. Cantatore, B. de Boer, P. W. M. Blom and D. M. de Leeuw, *Adv. Mater.*, 2006, **18**, 1900; (b) T. D. Anthopoulos, S. Setayesh, E. Smits, M. Cölle, E. Cantatore, B. de Boer, P. W. M. Blom and D. M. de Leeuw, *Adv. Mater.*, 2006, **18**, 1900.

5 (a) S.-i. Noro, H.-C. Chang, T. Takenobu, Y. Murayama, T. Kanbara, T. Aoyama, T. Sassa, T. Wada, D. Tanaka, S. Kitagawa, Y. Iwasa, T. Akutagawa and T. Nakamura, *J. Am. Chem. Soc.*, 2005, **127**, 10012; (b) S.-i. Noro, T. Takenobu, Y. Iwasa, H.-C. Chang, S. Kitagawa, T. Akutagawa and T. Nakamura, *Adv. Mater.*, 2008, **20**, 3399.

6 L.-L. Chua, J. Zaumsel, J.-F. Chang, E. C.-W. Ou, P. K.-H. Ho, H. Sirringhaus and R. H. Friend, *Nature*, 2005, **434**, 194.

7 (a) A. L. Balch and R. H. Holm, *J. Am. Chem. Soc.*, 1966, **88**, 5201; (b) Y. Konno and N. Matsushita, *Bull. Chem. Soc. Jpn.*, 2006, **79**, 1046.

8 A. Heaton, M. Hill and F. Drakesmith, *Journal of Fluorine Chemistry*, 1997, **81**, 133.

9 Parr, R. G.; Yang, W. *Density Functional Theory of Atoms and Molecules*; Oxford University Press: Oxford, 1989.

10 M. J. Frisch, G. W. Trucks, H. B. Schlegel, G. E. Scuseria, M. A. Robb, J. R. Cheeseman, G. Scalmani, V. Barone, B. Mennucci, G. A. Petersson, H. Nakatsuji, M. Caricato, X. Li, H. P. Hratchian, A. F. Izmaylov, J. Bloino, G. Zheng, J. L. Sonnenberg, M. Hada, M. Ehara, K. Toyota, R. Fukuda, J. Hasegawa, M. Ishida, T. Nakajima, Y. Honda, O. Kitao, H. Nakai, T. Vreven, J. A., Jr. Montgomery, J. E. Peralta, F. Ogliaro, M. Bearpark, J. J. Heyd, E. Brothers, K. N. Kudin, V. N. Staroverov, R. Kobayashi, J. Normand, K. Raghavachari, A. Rendell, J. C. Burant, S. S. Iyengar, J. Tomasi, M. Cossi, N. Rega, N. J. Millam, M. Klene, J. E. Knox, J. B. Cross, V. Bakken, C. Adamo, J. Jaramillo, R. Gomperts, R. E. Stratmann, O. Yazyev, A. J. Austin, R. Cammi, C. Pomelli, J. W. Ochterski, R. L. Martin, K. Morokuma, V. G. Zakrzewski, G. A. Voth, P. Salvador, J. J. Dannenberg, S. Dapprich, A. D. Daniels, Ö. Farkas, J. B. Foresman, J. V. Ortiz, J. Cioslowski, D. J. Fox, Gaussian 09 (Revision D.01), Gaussian, Inc., Wallingford CT, **2009**.

11 (a) D. Becke, *J. Chem. Phys.*, 1993, **98**, 5648; (b) C. Lee, W. Yang, R. G. Parr, *Phys. Rev. B*, 1988, **37**, 785.

12 R. Krishnan, J. S. Binkley, R. Seeger, J. A. Pople, *J. Chem. Phys.*, 1980, **72**, 650; (b) A. D. McLean, G. S. Chandler, *J. Chem. Phys.* 1980, **72**, 5639.

13 M. A. Thompson, ArgusLab 4.0.1; Planaria Software LLC: Seattle, WA, http://www.arguslab.com/arguslab.com/ArgusLab.html/.

14 V. Barone, M. Cossi, *J. Phys. Chem. A*, 1998, **102**, 1995; (b) M. Cossi, N. Rega, G. Scalmani, V. Barone, *J. Comp. Chem.*, 2003, **24**, 669.

15 (a) J. L. Bredas, R. Silbey, D. X. Boudreux, R. R. Chance, *J. Am. Chem. Soc.*, 1983, **105**, 10012; (b) A. Misra, P. Kumar, R. Srivastava, S. K. Dhawan, M. N. Kamalasanan, S.Chandra, *Indian. J. Pure Ap. Phy.*, 2005, **43**, 921.

16 Y. Konno and N. Matsushita, *Bull. Chem. Soc. Jpn.* 2006, **79**, 1237.

 